

1 Microbial resource management for *ex situ* 2 biomethanation of hydrogen at alkaline pH

3 Washington Logroño¹, Denny Popp¹, Sabine Kleinsteuber¹, Heike Sträuber¹, Hauke Harms¹, Marcell
4 Nikolausz^{1*}

5 ¹ Department of Environmental Microbiology, Helmholtz Centre for Environmental Research – UFZ, Leipzig,
6 Germany

7 * Correspondence: marcell.nikolausz@ufz.de; Tel.: +49 341 2434 566 (M.N.)

8 **Abstract:** Biomethanation is a promising solution to convert H₂ produced from surplus electricity and CO₂ to
9 CH₄ by using hydrogenotrophic methanogens. In *ex situ* biomethanation with mixed cultures, homoacetogens
10 and methanogens compete for H₂/CO₂. We enriched a hydrogenotrophic microbiota on CO₂ and H₂ as sole
11 carbon and energy sources, respectively, to investigate these competing reactions. Microbial community
12 structure and dynamics of bacteria and methanogenic archaea were evaluated through 16S rRNA and *mcrA*
13 gene amplicon sequencing, respectively. Hydrogenotrophic methanogens and homoacetogens were enriched
14 as acetate was concomitantly produced along with CH₄. By controlling the media composition, especially
15 changing the reducing agent, the formation of acetate was lowered and grid quality CH₄ (≥ 97%) was obtained.
16 Formate was identified as an intermediate that was produced and consumed during the bioprocess. Stirring
17 intensities ≥1000 rpm were detrimental, probably due to shear force stress. The predominating methanogens
18 belonged to the genera *Methanobacterium* and *Methanoculleus*. The bacterial community was dominated by
19 *Lutispora*. The methanogenic community was stable, whereas the bacterial community was more dynamic.
20 Our results suggest that hydrogenotrophic communities can be steered towards selective production of CH₄
21 from H₂/CO₂ by adapting the media composition, the reducing agent and the stirring intensity.

22 **Keywords:** power-to-gas, energy storage, biogas upgrading, biomethane, formate, hydrogenotrophic
23 methanogenesis, homoacetogenesis, *Methanobacterium*, *Methanoculleus*
24

25 1. Introduction

26 Renewable energy from wind power and photovoltaics increasingly leads to temporary excess of
27 electricity that cannot be handled by the grid and traditional storage infrastructure. Hence, technical solutions
28 to store this energy, e.g. in form of chemical energy carriers, are required. The power-to-gas (P2G) technology
29 converts surplus power into a storable gas [1]. H₂ can be generated through water electrolysis and subsequently
30 injected and stored in the natural gas grid, though with certain limitations [2]. Methane can also be produced
31 from excess electricity in a two-stage process: H₂ is first produced through water electrolysis and then used in
32 a methanation stage to reduce CO₂ to methane [2]. Although the H₂ production technology is quite advanced, it
33 has some drawbacks concerning long-term storage, safety and low energy density of H₂ as well as the
34 requirement of technical modifications of the natural gas grid. Methane, on the other hand, is very attractive
35 because the storage and distribution infrastructure is already in place in many countries. Methane can be readily
36 injected into the gas grid and has a volumetric energy content of 36 MJ m⁻³, which is more than three times
37 higher than that of H₂ (10.88 MJ m⁻³) [3].

38 Biogas is the product of anaerobic digestion (AD), which is a well-established commercial process and a
39 key technology in the current and future renewable energy sector [4]. Biogas consists mainly of CH₄ (40-75%)
40 and CO₂ (25-60%) and needs to be upgraded to biomethane by removing CO₂ if injection into the gas grid is
41 intended. Methods for biogas upgrading have been reviewed elsewhere [5–7]. Biological biogas upgrading
42 (biomethanation) uses external H₂ to convert the CO₂ share of the biogas into additional CH₄ via the CO₂-
43 reductive pathway of hydrogenotrophic methanogens. Biomethanation of H₂ is an emerging technology that
44 appears to be advantageous over the catalyst-based chemical methanation (Sabatier reaction) in terms of milder
45 reaction conditions [6]. This bioprocess can be performed by pure methanogenic strains [8] or mixed cultures
46 [6]. The latter may have certain economic and process advantages over pure cultures [9].

47 According to Kougiyas et al. [10] and Rittmann [11], biomethanation of H₂ can be done in three ways:
48 *in situ*, *ex situ* and by a hybrid process. In the *in situ* process, H₂ is injected into the main anaerobic digester or

49 post digester of a biogas plant to reduce CO₂ and thereby increase the CH₄ content of the biogas. In the *ex situ*
50 process, biogas or CO₂ reacts with H₂ in a bioreactor that is separate from the AD process. The hybrid process
51 couples partial biogas upgrading in the main AD reactor (*in situ*) with a final upgrading step in a separate reactor
52 (*ex situ*). Defining the system to be investigated according to the above mentioned categories is important for
53 comparisons in terms of efficiency and microbiota. An *ex situ* reactor could provide a defined ecological niche
54 to enrich specialized hydrogenotrophic microbiota with autotrophic metabolism (methanogenesis and
55 homoacetogenesis). It can be hypothesized that the inoculum, the operation temperature and the continuous
56 supply of H₂ play important roles in shaping the microbial community towards the predominance of either
57 hydrogenotrophic methanogens or homoacetogenic bacteria.

58 If a complex inoculum is used to perform *ex situ* biomethanation of H₂, acetate could be synthesized from
59 H₂ and CO₂ via the Wood-Ljungdahl pathway concomitantly with CH₄ formation. Acetate synthesis during *ex*
60 *situ* biomethanation represents a problem as it is an undesirable carbon and electron sink when CH₄ is the target
61 molecule. It is therefore necessary to manage the microbiota towards selective CH₄ production. In
62 environmental biotechnology, the term microbial resource management implies finding strategies to obtain and
63 maintain a highly performing community [12]. The understanding of metabolic processes in complex
64 communities imposes a great challenge that could be overcome by establishing enrichment cultures to
65 investigate the essential metabolic functions. Enrichment cultures are used to construct mixed culture metabolic
66 models and explore the ecophysiological functions of microbes that have not yet been isolated in pure culture
67 [13]. Enriched mixed cultures could be simple enough to investigate individual community members [14] and
68 represent opportunities to grow uncultivable microbes [15]. In fact, some microbes can only grow in the
69 presence of other microorganisms [16] and this could be true for the microorganisms of the AD microbiota that
70 still remains largely unexplored. In the *ex situ* H₂ biomethanation context, most studies resulted in the
71 enrichment of methanogens and homoacetogens. Previous *ex situ* biomethanation studies have found
72 *Methanobacteriales* [10,17–23], *Methanomicrobiales* [10,24] and *Methanococcales* [24] as the dominant
73 orders. *Methanothermobacter thermautotrophicus* was the dominant methanogen in three different reactor
74 configurations [10]. In the bacterial domain, *Firmicutes* [10,21,25,26], *Bacteroidetes* [10], *Synergistetes* [21]
75 and *Proteobacteria* [25] were the dominant phyla.

76 In previous studies, sludge from biogas reactors or wastewater anaerobic granules were used as inoculum
77 sources [10,17,19,24,27–31]. From the microbiological point of view, certain process parameters such as
78 temperature and pH, substrate characteristics and inoculum source define the community structure and
79 dominant members of the microbiota. An *ex situ* study comparing different reactor configurations reached
80 methane concentrations of more than 98%; however, acetic acid accumulated to concentrations of ~4 g L⁻¹ and
81 the pH values were ≥ 8 [10]. Similar pH values ranging from 7 to ≥ 8 were also reported in a continuous stirred
82 tank reactor (CSTR) for *ex situ* biomethanation [32]. Previous *ex situ* biomethanation studies have operated at
83 slightly alkaline pH, but microbial enrichment studies at such conditions are still missing.

84 In the present study, we explored *ex situ* biomethanation of H₂ at alkaline pH through an enrichment
85 process. The aim of the enrichment strategy was to better understand the microbial community dynamics
86 depending on the operational conditions as well as the competition between methanogenesis and
87 homoacetogenesis during *ex situ* biomethanation. According to previous studies, hydrogenotrophic
88 methanogenesis is the major methanogenic pathway under high nitrogen load and high ammonia concentration
89 [33–35]. Thus, we used the digestate of a laboratory-scale biogas reactor (CSTR) treating a nitrogen-rich
90 substrate (dried distillers grains with solubles, DDGS) as inoculum source for long-term enrichment of a
91 hydrogenotrophic microbiota that performs *ex situ* biomethanation. The experiments focused on the
92 characterization of the microbial community structure and dynamics during the enrichment by amplicon
93 sequencing of 16S rRNA and *mcrA* genes. Additionally, the effects of media components such as yeast extract
94 and reducing agent as well as of the stirring intensity on the H₂ and CO₂ metabolism were investigated.

95 2. Materials and Methods

96 2.1 Inoculum

97 Anaerobic sludge from a mesophilic (38°C) laboratory-scale CSTR treating DDGS was sieved using a
98 400-µm mesh size sieve under nitrogen flow. The liquid inoculum was degassed at 38°C for 7 days before use.

99 The basic characteristics are the mean values of triplicate measurements as follows: total solids (TS), 3.4%;
100 volatile solids (VS), 70.1%_{TS}; pH, 7.5.

101 2.2 Growth medium

102 Modified mineral medium DSMZ1036 containing yeast extract (0.2 g L⁻¹) as described previously [36]
103 was used for the enrichment and is designated as medium A in the following. For further experiments, the
104 medium was used in two variants: medium B did not contain yeast extract but was supplemented with a vitamin
105 solution as described by [37] and cysteine-HCl as reducing agent in the same concentration as in medium A.
106 Medium C contained vitamins like medium B but sodium sulfide as reducing agent as described by [37]. After
107 preparing the media as described in **Text S1**, the pH for all media variations was adjusted to 9 with a sterile
108 anoxic stock solution of 2 M KOH.

109 2.3 Enrichment setup

110 Strict anaerobic techniques were thoroughly applied in this study. Sterile anoxic bottles were prepared as
111 described in **Text S2** prior to medium dispensing and inoculation. The gas volume/liquid volume ratio was
112 maintained at 3 for all experiments regardless of the size of the bottle, unless stated otherwise. The experiments
113 were conducted with four biological replicates in the first stage (gas feeding of the anaerobic sludge) and
114 triplicates in the second stage (enrichment in mineral medium). The detailed chronology of the culture transfers
115 is provided in **Table S4**.

116 The setup in the first stage was assembled in an anaerobic chamber. Serum bottles of 219.5 mL volume
117 were filled with 50 mL degassed inoculum, sealed with butyl rubber stoppers and crimped with aluminum caps.
118 The gas phase of the serum bottles was replaced by H₂ (80%) and CO₂ (20%). All bottles receiving H₂ and CO₂
119 were operated in fed-batch mode and daily pressurized to ~2.2 bar for approximately five months. Bottles
120 containing the inoculum and a nitrogen atmosphere (not pressurized) were used as controls to account for the
121 residual biogas production. Detailed information about headspace flushing and pressurization is given in
122 **Text S2**.

123 In the second stage, medium A was used to enrich a particle-free culture by six subsequent culture transfers
124 in fresh medium bottles by inoculating the content of the previous culture transfer (10%, v/v). One randomly
125 selected replicate from the first stage served as inoculum to start the bottles of the second stage. Anoxic medium
126 A (45 mL) was dispensed to sterile, anoxic serum bottles and left overnight in an incubator at 37°C to reduce
127 any oxygen traces that entered the bottles during medium dispensing. Next, the bottles were inoculated with 5
128 mL culture from the first stage. Biological controls for determining residual biogas production (containing
129 inoculum but with N₂ gas phase) as well as sterile controls (not inoculated, but with either H₂/CO₂ or N₂ gas
130 phase) were also set up. The bottles were fed with gaseous substrate as described above and incubated at 37.4°C
131 in an orbital shaking incubator (IKA KS 4000 ic control, IKA®-Werke GmbH & Co. KG) at 200 rpm.

132 2.4 Cultivation experiments

133 In a series of four independent experiments, the effects of medium composition and stirring intensity on
134 biomethanation, biomass growth, and production of volatile fatty acids (VFA) were investigated. Experiments
135 were conducted in 1-L pressure-resistant Duran bottles (Schott AG, Germany). Bottles were inoculated with
136 10% (v/v) pre-culture (21 days old second stage enrichment culture, 11th transfer (T11)) and incubated at 37.4°C
137 under constant orbital shaking at 200 rpm. The experiments were conducted in duplicates and stepwise to
138 investigate the effect of the medium composition (media A, B and C as described in section 2.2). The gas
139 consumption and production as well as the development of biomass and VFA production were frequently
140 monitored.

141 After the optimal medium had been determined, we tested the effect of the stirring intensity on the CH₄
142 production and H₂/CO₂ consumption. Instead of shaking, the bottles were stirred with magnetic stirrers (top
143 plate diameter of 145 mm, speed range from 100 to 1,400 rpm; Heidolph, Germany) and new magnetic bars (50
144 mm × 8 mm, ABSOLUTE, Th. Geyer, Germany) and incubated at 38°C. To reduce detrimental effects of
145 shear forces on the cells, the liquid volume was increased to 500 mL, corresponding to a gas volume/liquid
146 volume ratio of 1. The experiments were conducted three times with duplicates (n=6).

147 Flushing and pressurizing as well as pressure determination and sampling of the gas and liquid phases
148 were done as described above (see also **Text S2**) for all four experiments.

149 2.5 Microbial community analysis

150 Samples for community analysis were taken from the inoculum (S) as well as after one month (1M) and 5
151 months (5M) fed-batch feeding during the first stage of the enrichment. Samples from the second stage were
152 taken at the end of the first (T1), third (T3), and sixth (T6) culture transfer. Liquid samples of 1.5 mL were
153 withdrawn from each bottle with a nitrogen-flushed syringe (**Text S2**) and centrifuged at 4°C and $20,817 \times g$
154 for 10 min. Pellets were stored at -20°C until DNA extraction. DNA was extracted with the NucleoSpin®Soil
155 Kit (MACHEREY-NAGEL GmbH & Co. KG, Germany) using buffer SL2 and enhancer solution. The quality
156 and quantity of extracted DNA were verified via gel electrophoresis (0.8% agarose) and photometrically using
157 a NanoDrop ND 1000 spectral photometer (Thermo Fisher Scientific, USA). Extracted DNA was stored at -
158 20°C until use. The microbial community composition was analyzed by amplicon sequencing of *mcrA* genes
159 for methanogens and 16S rRNA genes for bacteria.

160 In order to analyze the bacterial communities, the V3-V4 region of the 16S rRNA genes was amplified
161 using the universal primers 341f (5'-CCT ACG GGN GGC WGC AG-3') and 785r (5'-GAC TAC HVG GGT
162 ATC TAA KCC-3') described by Klindworth et al. [38]. For the analysis of the methanogenic communities,
163 the *mlsA* (5'-GGT GGT GTM GGD TTC ACM CAR TA-3') and *mcrA*-rev (5'-CGT TCA TBG CGT AGT
164 TVG GRT AGT- 3') primers were used as described previously [39]. All primers contained Illumina MiSeq-
165 specific overhangs. Amplicon libraries were prepared and sequenced on the Illumina MiSeq platform using the
166 MiSeq Reagent Kit v3 with 2x300 cycles. Demultiplexed raw sequence data were deposited at the EMBL ENA
167 under the study accession number PRJEB36972 (<http://www.ebi.ac.uk/ena/data/view/PRJEB36972>).

168 Primer sequences were clipped from demultiplexed and adapter-free reads using Cutadapt v1.18 [40].
169 Further sequence analysis was performed using QIIME2 v2019.1 [41]. Sequences were trimmed, denoised and
170 merged using the dada2 plugin [42]. For 16S rRNA gene analysis, forward and reverse reads were truncated at
171 270 bp and 240 bp, respectively. For *mcrA* gene analysis, reads were truncated at 270 bp and 230 bp,
172 respectively. Maximum expected errors were set to 2, which is the default value. Chimeras were removed in
173 default consensus mode of the dada2 plugin. Resulting feature sequences of 16S rRNA gene analysis were
174 classified against the MiDAS database v2.1 [43] trimmed to the region covered by the 341f and 785r primers.
175 For *mcrA* gene analysis, a taxonomy database was created by using *mcrA* sequences from the RDP FunGene
176 database [44]. For this purpose, *mcrA* sequences were downloaded (2,878 sequences on 21st January 2019),
177 sequences from uncultured organisms and metagenomic sequences were removed, and taxonomic information
178 was formatted resulting in 385 sequences used for the classification. As the primer combination 341f/785r also
179 amplifies archaeal 16S rRNA genes, archaeal reads were removed from further analysis of the 16S rRNA genes
180 and bacterial read counts were normalized to 100%.

181 2.6 Analytical methods

182 To determine the TS content of the inoculum, samples were dried at 105°C for 24 h and the mass was
183 recorded. The TS value was calculated from the mass difference of the fresh and dried sample. Subsequently,
184 the samples were incinerated at 550°C in a muffle furnace for 2 h and the mass was recorded. The VS value
185 was calculated based on mass difference of dried and incinerated samples. The mean values of triplicate
186 measurements are presented.

187 To determine the headspace gas composition, 1 mL gas sample was withdrawn with a syringe and injected
188 into an argon pre-flushed glass vial of 20 mL (**Text S2**). The gas samples were measured via gas
189 chromatography equipped with an autosampler in a Perkin Elmer GC. The GC was equipped with HayeSep N
190 / Mole Sieve 13X columns and a thermal conductivity detector. The oven and detector temperatures were 60°C
191 and 200°C, respectively. The carrier gas was argon. Every gas sample was analyzed immediately or within 24
192 h after sampling.

193 The relative pressure in the bottles was measured with a digital manometer (**Text S2**). The gas amount in
194 the bottles was calculated according to Equation 1 (Eq. 1). Standard conditions were considered for calculations
195 ($P = 1.01325$ bar, $T = 298.15$ K). The consumption and production rates of gases (H_2 , CO_2 , and CH_4) were
196 determined from the linear slope of at least three continuous measurements and are given in mmol gas per liter
197 liquid volume per hour ($mmol L^{-1} h^{-1}$).

$$Gas_{(Xi)}[mmol] = \frac{P_{abs}[mbar] \times \frac{Gas_{(Xi)}[\%]}{100} \times V_h[mL]}{R \times T[K]} \times 1000 \quad \text{Eq. 1}$$

198

199

200

201

202

203

204

205

206

207

208

209

210

211

212

213

214

Where, Xi refers to the gas in question, P_{abs} is the absolute pressure inside the bottle, V_h is the headspace volume of the cultivation bottle (169.5 mL), R is the universal gas constant (8.314×10^4 mbar cm³ mol⁻¹ K⁻¹), and T is the standard temperature.

For measuring the concentration of VFA (formic, acetic, propionic and butyric acid), the supernatants from liquid samples were filtered through a membrane filter with 0.2 μm pore size (13 mm; LABSOLUTE, Th. Geyer GmbH, Germany) and stored at -20°C or analyzed immediately. When needed, appropriate dilutions were prepared with deionized water and the samples were analyzed by using high performance liquid chromatography (HPLC; Shimadzu Scientific Instruments, US) equipped with an RID detector L-2490 and an ICSep column COREGEL87H3 (Transgenomic Inc., USA). The sample volume for HPLC measurement was 200 μL and the injection volume was 20 μL. The HPLC measurements were done with 5 mM H₂SO₄ as eluent at a flow rate of 0.7 mL min⁻¹.

The pH value of the broth was measured in 200 μL liquid samples using a mini-pH meter (ISFET pH meter S2K922, ISFETCOM Co., Ltd., Japan) and the value was recorded after 90 s. For particular experiments with medium B and C, the pH was determined as aforementioned after a centrifugation step at $20,817 \times g$, 4°C, 10 min.

215

2.7 Statistical analysis

216

217

218

219

220

221

222

223

The methane concentrations of the two stages were compared when the gas conversion and production was stable throughout several feeding cycles (variation was less than 10% in at least ten consecutive batch-cycle feedings) by means of analysis of variance (ANOVA). A Tukey post-hoc test was used for multiple comparisons with a confidence level of 0.05. RStudio [45], Graphpad (Graphpad Software, Inc., San Diego, CA) or Microsoft Excel were used to compute the data. Microbial community composition data were analyzed by principal coordinate analysis (PCoA) based on Bray-Curtis distances of relative abundances in addition to the absence and presence using the phyloseq package [41] version 1.30.0 in R [46] version 3.6.1. PCoA was plotted using the ggplot2 package [47] version 3.2.1.

224

3. Results and Discussion

225

3.1 Enrichment of the hydrogenotrophic community and biomethanation performance

226

227

228

229

230

231

232

233

During the first stage of the enrichment, methane was formed within 24 h upon H₂/CO₂ feeding, and the process was stable for ~5 months. The rapid gas substrate conversion indicated high hydrogenotrophic methanogenesis activity in the inoculum. This observation is in agreement with a previous study [48]. However, the highest methane concentration between feeding cycles was only ~90% (**Figure S1**). In the second stage of the enrichment, the CH₄ concentrations in six successive transfers (T1-T6) were as high as in the bioreactors working with sludge in the first stage (**Table 1**). The CH₄ concentration was 6% lower than the one described in a previous study [17] but similar to that observed in another previous study [20].

Particle-free cultures were obtained after the third transfer and therefore the cell biomass from T3-T6 could be followed by spectrophotometry via optical density (OD₆₀₀) (**Figure S2**). On average, each transfer from T3 to T6 started with a biomass of 91 ± 22 mg L⁻¹ whereas the final biomass was on average 579 ± 26 mg L⁻¹. In terms of biomass and gas composition no significant difference ($p \leq 0.05$) among transfers was found when comparing the end points of each transfer (**Table 1**). At the end of each culture transfer, the pH was ~8, a value similar to that reported in a previous study [10]. Acetate was found in considerable concentrations from T1 to T5 but not in the seed sludge (after ~5 months) and in T6 (see **Table 1**), indicating that homoacetogenesis was a concomitant reaction along with methanogenesis in our enriched hydrogenotrophic community. The variation in acetate concentrations among transfers could be associated with the cultivation time, especially for the particle-free enrichment cultures (T5 and T6), where the acetate concentration was generally low and the cultivation time was long.

244

245

246

The decrease of the acetate concentration at the end of the culture transfer (T6) suggests decreased homoacetogenic activity or increased acetate utilization via syntrophic acetate oxidation (SAO) since acetotrophic methanogens were absent in our enrichment cultures (see section 3.2). Another explanation for the

247 decrease could be acetate assimilation to build up microbial biomass since hydrogenotrophic microbes can use
248 an organic carbon source such as acetate when available. It was previously reported that acetate is central to the
249 carbon metabolism of autotrophic and heterotrophic microbes [49]. Despite the variations of acetate
250 concentration, the observed values throughout the culture transfers were similar to those reported in other
251 studies [10,19,24,26,30]. Since acetate was the main side product, the kinetics of acetate consumption was
252 assessed in more detail during one batch-cycle feeding when the culture (T1) presented stable gas consumption
253 in several consecutive batch cycles (**Figure S3**). Acetate was consumed during the first 7 h (4% consumption
254 likely to build biomass) and then its concentration increased again (1% increase), although the final
255 concentration was 3% less than the initial concentration. Propionate and butyrate were also detected and the
256 highest concentrations were found in T1 and T3. However, their concentrations decreased over the consecutive
257 transfers (**Table 1**). Most likely this effect was also related to the cultivation time of the culture transfers.

258

Table 1. Summary of process parameters during the enrichment in the first stage with sludge and in the second stage with six culture transfers (T1-T6).

Sample	Sludge ^b	T1 ^c	T2 ^c	T3 ^c	T4 ^c	T5 ^c	T6 ^c
Days of incubation	167	56	27	22	24	28	40
CH ₄ (%) ^a	85.17 ± 4.5	86.99 ± 5.4	88.04 ± 3.2	87.48 ± 4.7	88.00 ± 2.3	87.21 ± 4.1	87.47 ± 2.5
Biomass concentration start (mg L ⁻¹) ^d	-	-	-	92.2 ± 11.73	91.4 ± 2.56	90.3 ± 17.79	88.6 ± 10.48
end (mg L ⁻¹) ^d	-	-	-	609.1 ± 33.57	548.2 ± 30.22	570.7 ± 31.46	588.2 ± 32.42
pH (start)	8.0 ± 0.1	9.0 ± 0.1	9.0 ± 0.1	9.0 ± 0.1	9.0 ± 0.1	9.0 ± 0.1	9.0 ± 0.1
pH (end)	8.5 ± 0.2	8.4 ± 0.1	8.3 ± 0.2	7.9 ± 0.1	8.1 ± 0.1	8.0 ± 0.1	8.1 ± 0.1
Acetate (mg L ⁻¹)	123.5 ± 7.8	2089 ± 194	970.8 ± 54.6	1922 ± 398	2053 ± 156	886.9 ± 170.9	122.7 ± 20.1
Propionate (mg L ⁻¹)	0.0 ± 0.0	26.03 ± 2.3	492.1 ± 16.4	185.9 ± 18.3	188.3 ± 37.9	135.9 ± 3.9	92.15 ± 3.7
Butyrate (mg L ⁻¹)	0.0 ± 0.0	56.33 ± 19.2	0.0 ± 0.0	147.2 ± 13.2	84.04 ± 10.26	28.1 ± 0.84	25.89 ± 1.4

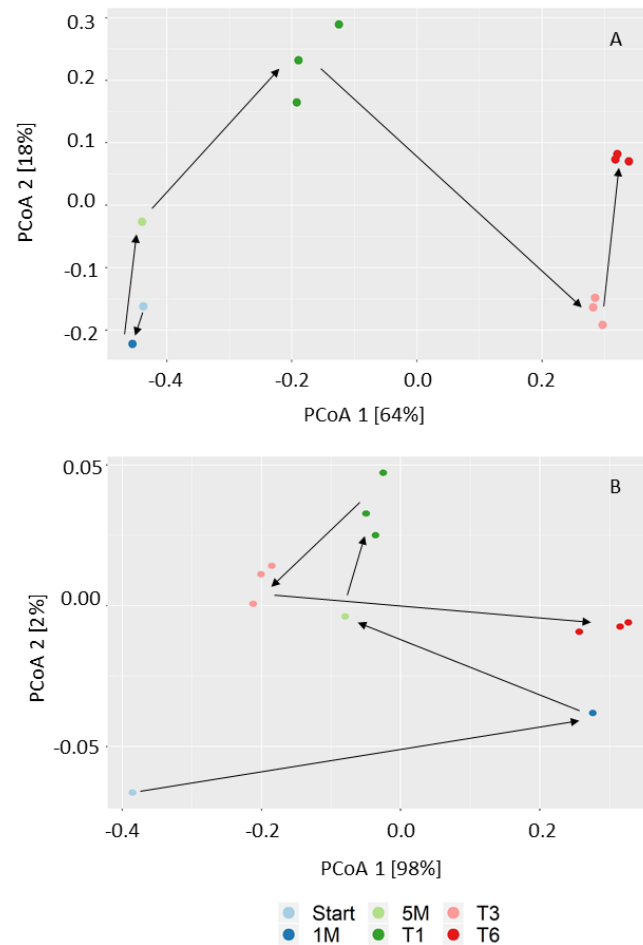
259 ^a Concentration measured when the gas production was stable (mean and standard deviation, n=17).260 ^b Four biological replicates. Mean and standard deviation is shown.261 ^c Three biological replicates. Mean and standard deviation is shown262 ^d Experimental conversion factor for biomass quantification: 1 OD₆₀₀ = 0.423 g L⁻¹ dry weight. Details are given in **Figure S3**.

263

264

265 3.2 Microbial community structure and dynamics

266 Feeding the complex community with a rather simple substrate has probably reduced the microbial
267 diversity as shown previously [10] but it could still maintain a number of cooperative as well as competing
268 functional groups. The effect of H₂/CO₂ as selection factor shaping the bacterial and methanogenic communities
269 resulted in a dynamic process throughout the enrichment as visualized by PCoA (see time trajectory in
270 **Figure 1**). The first two axes explained 64% and 98% of the variance for the bacterial (**Figure 1A**) and
271 methanogenic (**Figure 1B**) communities, respectively. Hence, a two-dimensional plot is sufficient to represent
272 the relation between the samples. Microbial communities grouped according to transfers, which means that the
273 communities of the same transfer were quite similar but different from those of the other transfers.



274

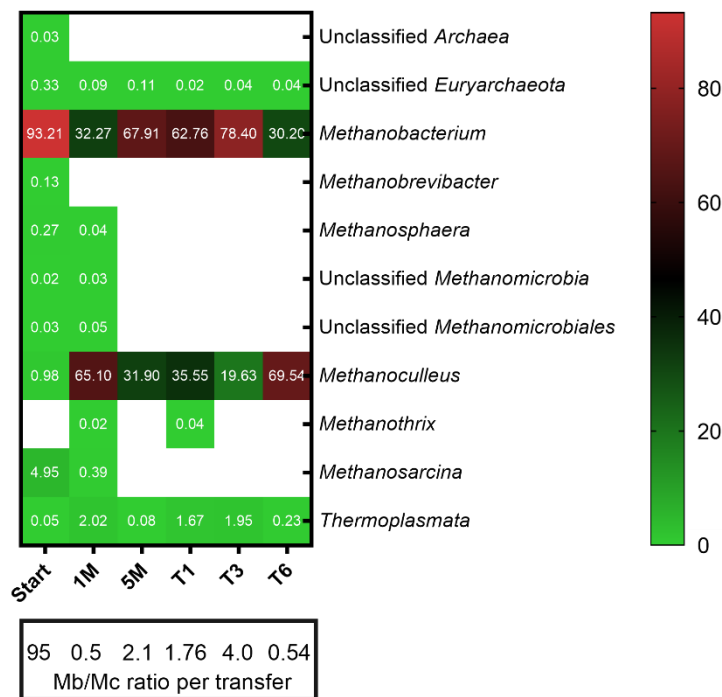
275 **Figure 1.** Principal coordinate analysis (PCoA) based on Bray-Curtis distances showing the microbial
276 community shift during the enrichment. A) Bacterial community (16S rRNA gene amplicon sequences) and B)
277 methanogenic community (*mcrA* gene amplicon sequences). The labels of the figure are as follows: inoculum
278 (Start), one month (1M), 5 months (5M) after fed-batch feeding during the first stage; first transfer (T1), third
279 transfer (T3), and sixth transfer (T6) after fed-batch feeding in the second stage.

280 As expected based on the high ammonia level (5.84 g L⁻¹ NH₄-N) of the source digester, the methanogenic
281 community in the inoculum was dominated by hydrogenotrophic methanogens affiliated to the genus
282 *Methanobacterium* (**Figure 2**), which is in agreement with previous studies on high ammonia level reactors
283 [33–35]. Methanogens affiliated to the genus *Methanosarcina* were also present in the inoculum but disappeared
284 after one month of H₂/CO₂ feeding despite their versatility in substrate utilization. It was proposed that H₂
285 feeding exerts a selection pressure to enrich hydrogenotrophic methanogens [21,25], which could explain the

286 disappearance of *Methanosarcina* and the complete dominance of strictly hydrogenotrophic methanogens in
 287 the enrichment. Furthermore, the H₂ uptake rate was reported to be one order of magnitude higher for the strict
 288 hydrogenotrophic methanogen *Methanococcus maripaludis* [50] than for the versatile methanogen
 289 *Methanosarcina barkeri* [51], thus considering this aspect may also explain why *Methanosarcina* disappeared
 290 although it can grow on H₂/CO₂.

291 Species of the genus *Methanoculleus* dominated (65% of the total methanogenic community) after one
 292 month of fed-batch feeding of H₂/CO₂ but decreased to 32% after 5 months during the first stage of the
 293 enrichment. In the second stage, *Methanobacterium* dominated the methanogenic community in the inoculum
 294 (5M) but after H₂/CO₂ fed-batch feeding *Methanoculleus* increased in relative abundance and eventually
 295 became the dominant methanogen (T6). Previous studies reported *Methanoculleus* [25] and *Methanobacteriales*
 296 as the dominant methanogenic taxa [17] regardless of the reactor configuration. Members of the order
 297 *Methanomassiliicoccales* (class *Thermoplasmata* **Figure 2**) were present until the end of the experiment with
 298 low relative abundance, similar to a previous *ex situ* biomethanation study [26].

299 In reactors operated under thermophilic conditions ($\geq 55^{\circ}\text{C}$), *Methanothermobacter* and *Methanoculleus*
 300 dominated the methanogenic community as indicated in previous studies [10,24,25,52]. Consequently, we
 301 suggest that regardless of the operational temperature, methanogens affiliated to the *Methanomicrobiaceae* and
 302 *Methanobacteriaceae* seem to be key players of *ex situ* biomethanation processes since both families dominated
 303 the methanogenic community of our enrichment culture.

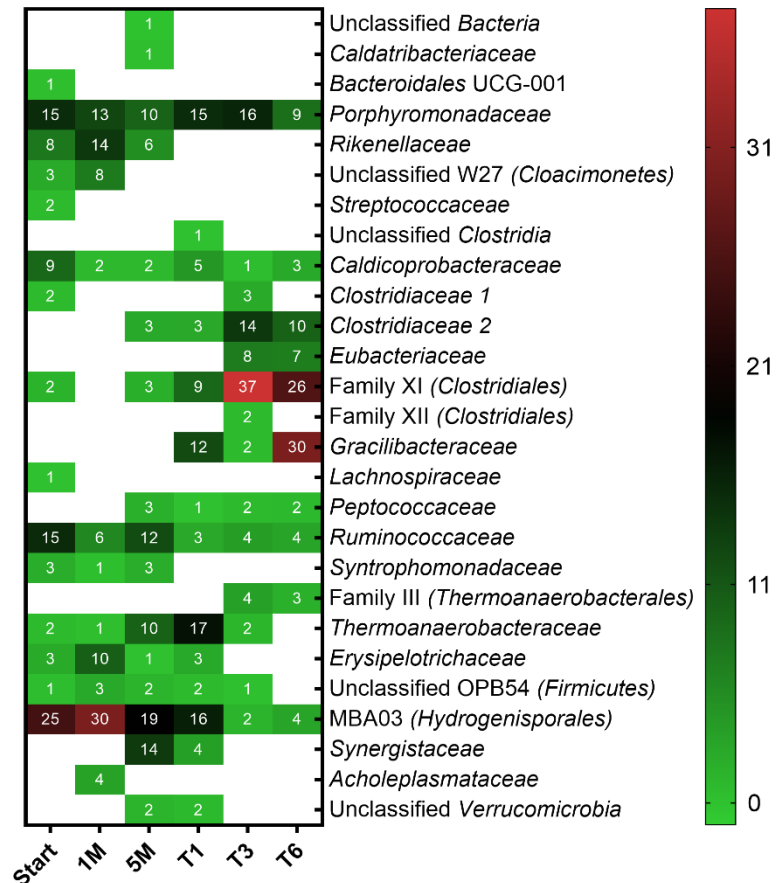


304

305 **Figure 2.** Methanogenic community structure in different stages of the enrichment. Taxa with a relative
 306 abundance less than 0.01% were filtered out from all samples. Numbers represent the relative abundance in
 307 percent and blank space indicates the absence of the respective taxa. The ratio of the most dominant
 308 methanogens *Methanobacterium* (Mb) and *Methanoculleus* (Mc) among transfers is shown. Mean values of
 309 three biological replicates are presented for T1, T3 and T6 whereas single values are shown for Start, 1M and
 310 5M.

311 The bacterial community was an integral part of the microbial community because VFA were produced
 312 and consumed (**Table 1**). Mainly acetate formation and consumption was observed, which indicates
 313 homoacetogenesis and SAO. At the end of the enrichment (T6) the dominant phylum was *Firmicutes* (91%)
 314 (**Figure S4**), which is consistent with previous findings [21], followed by the phylum *Bacteroidetes* (9%).
 315 Cooperation and competition can be expected in H₂ biomethanation systems since the microbial community
 316 can be composed of hydrogenotrophic and acetotrophic methanogens, homoacetogenic bacteria, and syntrophic
 317 acetate-oxidizing bacteria (SAOB) [10,25] as well as chain-elongating, predatory and scavenger

318 microorganisms. In the present study, acetotrophic methanogens were not present due to a mainly
 319 hydrogenotrophic seed sludge. In general, it is conceivable that strict acetotrophic methanogens (*Methanotherix*)
 320 coexist with homoacetogens in hydrogenotrophic communities. While a lower abundance of *Firmicutes* was
 321 described previously [10,23], a similar abundance as in this study was found by other studies [25,52,53]. In
 322 contrast, *Bacteroidetes* was found as dominant phylum by another study [54].



323

324 **Figure 3.** Bacterial community structure in different stages of the enrichment. Taxa with relative abundances
 325 less than 1% were filtered out from all samples. Numbers represent the relative abundance in percent and blank
 326 spaces indicate the absence of the respective taxa. Mean values of three biological replicates are presented for
 327 T1, T3 and T6 whereas single values are shown for Start, 1M and 5M.

328 Throughout the enrichment, the abundance of the class *Clostridia* increased to 86% in the sixth transfer
 329 (**Figure S5**), whereas the classes *Bacteroidia* and OPB54 (*Firmicutes*) that were dominant in the inoculum
 330 decreased in relative abundance to 9% and 5%, respectively (**Figure S5**). The production of acetate from
 331 H₂/CO₂ (Table 1) indicated homoacetogenesis, which can be attributed to members of the *Clostridiales* that
 332 dominated the bacterial community throughout the enrichment (**Figure S6**). Some members of this order are
 333 crucial for homoacetogenesis [55] or SAOB [56]. Homoacetogens and SAOB use the Wood-Ljungdahl pathway
 334 in the reductive or oxidative direction to produce acetate from CO₂ or to oxidize acetate to CO₂, respectively
 335 [55,57,58].

336

337 Mesophilic acetogens belong predominantly to the orders *Clostridiales* and *Selenomonadales* whereas
 338 thermophilic acetogens belong to the order *Thermoanaerobacterales* [59]. *Clostridiales* and
 339 *Thermoanaerobacterales* were both present in the enrichment culture (**Figure S6**) and together with the
 340 detection of acetate (**Table 1**) indicate the presence of acetogenic bacteria.

341

342 It is notable that in T6 *Lutispora* was the predominant genus with a relative abundance of 31% (**Figure**
343 **S7**). The only described species of this genus is a thermophile not known to be a homoacetogen, which suggests
344 novel homoacetogenic species may be present in the enrichment culture and supports the need to further explore
345 such unknown microbiota. This genus belongs to the clostridial family *Gracilibacteraceae*, which was found
346 in low relative abundance in a previous biomethanation study [26]. Other genera such as MBA03
347 (*Hydrogenisporales*) (19%), unclassified Family XI (*Clostridiales*) (15%), *Natronincola* (10%), unclassified
348 *Rikenellaceae* (11%), *Fastidiosipila* (8%), *Garciella* (7%), and *Petrimonas* (5%) were also abundant parts of
349 the bacterial community (**Figure S7**).

350

351 The acetate consumption could have occurred via SAO (e.g., by members of the classes *Synergistia* or
352 OPB54 (*Firmicutes*) [60]) or was assimilated by acetogens and hydrogenotrophic methanogens to build
353 biomass. The order *Thermoanaerobacterales* (class *Clostridia*) was present in lower abundance (3% in T6) with
354 a dynamic behavior in the second stage reaching similar levels as in the inoculum. Within this order, bacteria
355 affiliated to the genus *Gelria* (family *Thermoanaerobacteraceae*) were found. This family comprises two
356 species known as SAOB (*Thermacetogenium phaeum* and *Tepidanaerobacter acetatoxydans*), and *Gelria* was
357 also suggested to be involved in SAO [61]. Although the relative abundance of this genus decreased drastically
358 towards T6, a syntrophic association with the two most dominant methanogens (*Methanoculleus* and
359 *Methanobacterium*) of the enrichment culture is conceivable. Hence, the low concentration of acetate,
360 especially in T6 (~123 mg L⁻¹) could be explained by the activity of SAOB or high acetate assimilation by the
361 microbial community. The SAO function of the enrichment culture might be a shared task carried out by
362 different phylotypes since the biggest difference in abundances of *Gelria* and *Tepidanaerobacter* genera was
363 observed at the end of T1. A previous study found *Tepidanaerobacter syntrophicus* in an *ex situ* biomethanation
364 setup and suggested this species to be responsible for SAO [21]. Further investigations are needed by combining
365 different omics approaches with improved isolation attempts to explore the largely unknown function of
366 microorganisms represented only by sequence data.

367 3.3 Microbial resource management for selective production of methane

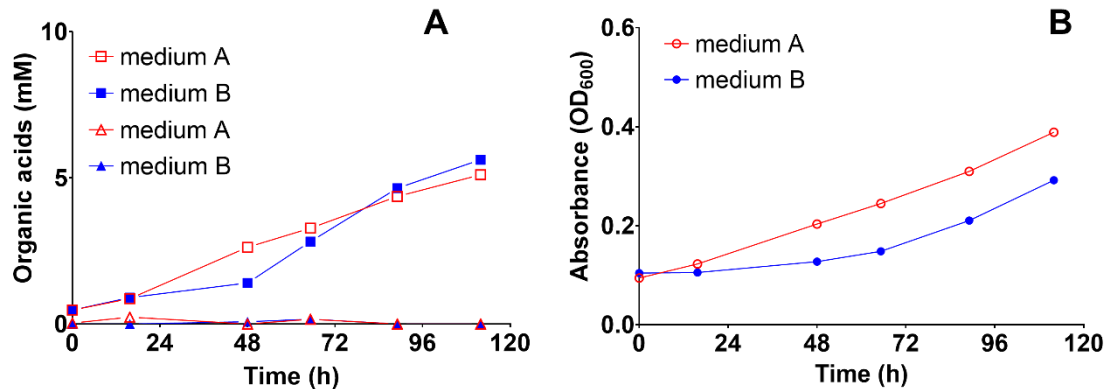
368 3.3.1 Effect of medium composition

369 Our *ex situ* biomethanation experiment concomitantly enriched homoacetogenic bacteria and
370 hydrogenotrophic methanogens similar to previous studies [10,19,24,30]. It was argued that operational
371 conditions are crucial to shape the microbial community composition that ultimately would lead to a maximized
372 methane yield [26]. Such control of parameters falls into the concept of microbial resource management for
373 selective production of any desired target molecule [12,62]. Here, we showed that selective methane production
374 with enrichment cultures that contain both homoacetogenic bacteria and hydrogenotrophic methanogens is
375 possible by controlling the medium composition. We explored the effect of several medium components on the
376 products of the hydrogenotrophic enrichment culture in a separate set of experiments with a focus on the
377 products (CH₄ and VFA) and not the microbial community. The inocula for these experiments were derived
378 from the last culture transfer of the enrichment phase (T11).

379 First, we assessed the effect of yeast extract in a medium containing cysteine-HCl as reducing agent by
380 comparing cultivation in mineral medium with (medium A) or without yeast extract (medium B). Acetate was
381 produced up to ~5 mM in both media whereas formate was not produced at all (**Figure 4A**). However, medium
382 A yielded 25% more biomass than medium B after the first batch-cycle feeding ($p = 0.0031$), even though the
383 yeast extract concentration was as low as 0.25 mg L⁻¹ (**Figure 4B**). A cultivation broth with such low
384 concentration of yeast extract is considered as mineral medium [63].

385

386



387

388

389

390

391

392

393

394

Figure 4. The effect of yeast extract on the production of acetic and formic acid and biomass during autotrophic feeding with H₂/CO₂ (80:20) in a 1-L bioreactors with medium A (containing 0.2 g L⁻¹ yeast extract) and medium B (free of yeast extract but containing vitamins). Both media were reduced with cysteine-HCl. (A) Acetic acid and formic acid concentration profiles during the first batch cycle, and (B) microbial biomass growth as measured by optical density at 600 nm during the first batch cycle. The experiments were conducted in two biological replicates with orbital shaking at 200 rpm. Each data point depicts the median and range (invisible error bars are smaller than the symbol). Square: acetic acid, triangle: formic acid, circle: biomass.

395

396

397

398

399

400

401

402

403

404

405

406

407

408

409

410

411

412

413

414

415

416

417

418

419

420

421

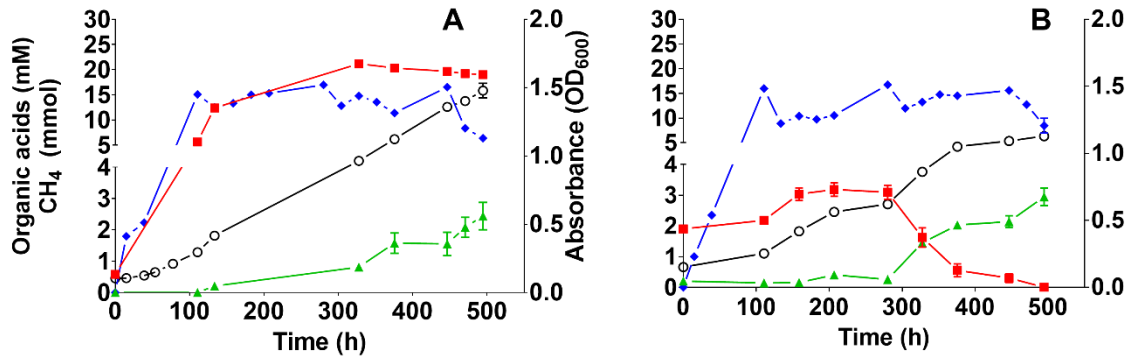
422

423

424

425

In a second experiment, we tested the effect of the reducing agent on VFA formation in medium B (containing cysteine-HCl as reducing agent) and medium C (containing sodium sulfide as reducing agent). Acetate accumulated in both cultures with medium B and C but after ~300 h the concentration started to decrease and concomitantly formate concentration started to increase (**Figure 5**). This observation could indicate that formate formation resulted from acetate degradation and could be related to SAO (involving interspecies formate transfer). However, the possibility of direct formate production from H₂/CO₂ cannot be ruled out. The acetate concentration in medium B was as high as 20 mM (**Figure 5A**) whereas incubation for ~500 h in medium C yielded no acetate (**Figure 5B**). If cysteine-HCl is taken into account as an additional carbon source, up to 3.42 mM acetate is expected, which is far less than the accumulated acetate concentration in medium B (**Figure 5A**), suggesting that acetate was mainly produced from H₂/CO₂. The final formate concentrations after 500 h were 2.4 and 2.9 mM in the cultures with medium B and C, respectively (**Figure 5**). After 500 h of operation, when the batch-cycle feeding was stopped, formate was rapidly consumed (data not shown). To our knowledge, experimental evidence of formate production in *ex situ* biomethanation has not been reported hitherto. Indeed, formate is an alternative electron donor for hydrogenotrophic methanogens [64]. Moreover, a previous study showed formate synthesis from H₂/CO₂ in bacteria [65]. Furthermore, pure cultures of hydrogenotrophic methanogens (*Methanobacterium formicicum*) or acetogenic bacteria transiently produced formate during H₂/CO₂ metabolism [66,67]. Hence, it can be inferred that homoacetogens, SAOB and hydrogenotrophic methanogens could have contributed to the concomitant formate formation along with methanogenesis. The observed formate concentration could be the result of dynamic production and consumption. The measurement of formate in micromolar concentrations is rather difficult [64]. This might explain why formate has not been reported in the liquid products in previous studies on *ex situ* biomethanation. Altogether, the results confirmed that formate was an intermediate during *ex situ* biomethanation; however, the exact mechanisms are still unclear. Reducing the sampling time intervals was important to allow formate determination in the broth. Biomass growth increased until the end of the experiment with medium B, whereas a plateau was reached after ~375 h with medium C (biomass concentration in medium B was 24% higher than in medium C). This may be explained by sulfur depletion after prolonged incubation in medium C because the medium was not replenished during the experimental period (the sulfur concentrations in medium B and C were 0.374 and 0.208 mM, respectively). The depletion of trace elements, which causes process imbalances because they are essential in enzyme complexes [68], may also explain the decreased methane production in both media after prolonged incubation. Although the biomass was less in medium C, the CH₄ concentration was higher than in medium B (32.5%).

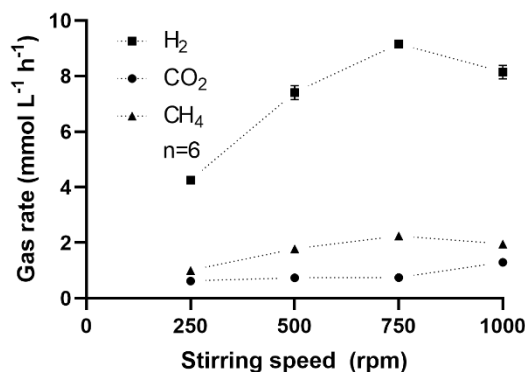


426

427 **Figure 5.** Effect of the reducing agent on the anaerobic conversion of H₂/CO₂ (80:20; fed-batch) in 1-L
 428 bioreactors shaking at 200 rpm. (A) Medium B (mineral medium free of yeast extract, supplemented with
 429 vitamins and reduced with cysteine-HCl), and (B) medium C (prepared as medium B but containing sodium
 430 sulfide instead of cysteine-HCl as reducing agent; see section 2.2). The experiments were conducted in two
 431 biological replicates and each data point depicts the median and range. Red square: acetic acid (mM), green
 432 triangle: formic acid (mM), blue diamond: CH₄ (mmol), and black open circle: biomass.

433 3.3.2 Effect of stirring intensity

434 Next, the effect of the stirring intensity on the methane formation rate was analyzed. Improved mixing
 435 was reported to enhance the gas mass transfer and hence methane formation rate [3,17]. As shown in **Figure 6**,
 436 the methane formation rate increased proportionally with the stirring intensity up to a maximum of ~9 mmol L⁻¹ h⁻¹
 437 at 750 rpm. However, in this particle-free enrichment culture growing in a mineral medium, further
 438 increasing the stirring intensity to ≥1000 rpm was detrimental (**Figure 6**) for both methane formation and H₂
 439 consumption rates. Although shaking exerts a different type of mixing than stirring does, our results are in line
 440 with a previous study where shaking intensities of 200-250 rpm were already detrimental for biomethanation
 441 performed with sludge [28]. On the contrary, an *in situ* biomethanation study working with sludge reported
 442 improved gas mass transfer with a stirring intensity as high as 1000 rpm [69]. This indicates that sludge can
 443 better resist shear forces caused by high stirring intensity than enrichment cultures, so that selecting a proper
 444 mixing intensity is dependent on the type of the liquid matrix used as biocatalyst. Under optimal conditions,
 445 the enrichment culture was capable of consuming the gaseous substrate within 24 h or less, similar to times reported
 446 elsewhere [17,70]. It is to note that high shear (stirring speed ≥ 1000 rpm) may have a negative effect on the
 447 syntrophic interactions between bacteria and methanogens.
 448



449

450 **Figure 6.** Effect of the stirring intensity on the consumption and formation rate of gases in a 1-L bioreactor with
 451 medium C. Bottles were pressurized at ~2.2 bar with a gas mixture of H₂ (80%) and CO₂ (20%). The rate for
 452 each stirring speed was repeated three times in duplicate biological bioreactors. Mean and standard deviation
 453 (n=6) is shown (invisible error bars are smaller than the symbol).

454 With an optimized medium composition (medium C) and mixing intensity (750 rpm), we obtained $\geq 97\%$
455 methane in the gas phase, which is comparable to previous studies [1,6]. Although other measures may also
456 affect the process performance, microbial resource management for biomethanation seems to be important when
457 enriched mixed cultures are used as biocatalysts.

458 4. Conclusions

459 We showed the enrichment of a hydrogenotrophic community that successfully produced grid quality
460 methane ($\geq 97\%$) through *ex situ* biomethanation. The methanogenic community was dominated by
461 *Methanoculleus* and *Methanobacterium*. Microbial resource management allowed the control of
462 homoacetogenesis by directing the carbon and electron flows towards selective methane production by carefully
463 defining the medium composition. The reducing agent played a pivotal role in controlling the production of
464 acetate, while too high stirring intensities negatively affected *ex situ* biomethanation in a particle-free highly
465 enriched community. Several bacterial taxa could be responsible for homoacetogenesis (mainly *Clostridia*).
466 Thus, further investigations are needed to elucidate the physiological role of the most abundant bacterial genera
467 in the hydrogenotrophic community.

468 **Supplementary Materials:** Text S1: Media composition, Text S2: Chemicals and experimental operation, Text S3:
469 Chronology of the culture transfers, Table S1. Composition of the medium component 1, Table S2. Stock solutions used to
470 supplement the media for different experiments, Table S3. Composition of stock solutions, Table S4 Chronology of culture
471 transfers, Figure S1 Methane concentrations during successive culture transfers in medium A, Figure S2 Correlation between
472 optical density and biomass concentration, Figure S3 Acetate concentration profile during one batch cycle feeding with T1,
473 Figure S4 Bacterial relative abundance at phylum level for different stages of the enrichment, Figure S5 Bacterial relative
474 abundance at class level for different stages of the enrichment, Figure S6 Bacterial relative abundance at order level for
475 different stages of the enrichment, Figure S7 Bacterial relative abundance at genus level for different stages of the
476 enrichment.

477 **Author Contributions:** Conceptualization: W.L., S.K. and M.N.; Methodology: W.L., D.P., H.S. and M.N.; Investigation:
478 W.L.; Formal analysis: W.L. and D.P.; Data curation: W.L. and D.P.; Writing – Original Draft Preparation: W.L.; Writing
479 – Review & Editing: D.P., S.K., H.S., H.H. and M.N.; Visualization: W.L.; Supervision: S.K., H.H. and M.N.; Project
480 Administration: S.K. All authors have read and approved the final manuscript.

481 **Funding:** This research received no external funding.

482 **Acknowledgments:** Ute Lohse is duly acknowledged for technical assistance in library preparation for MiSeq amplicon
483 sequencing. Cloud computing facilities used for the analysis of the amplicon were provided by the BMBF-funded de.NBI
484 Cloud within the German Network for Bioinformatics Infrastructure (de.NBI) (031A537B, 031A533A, 031A538A,
485 031A533B, 031A535A, 031A537C, 031A534A, 031A532B).

486 **Conflicts of Interest:** The authors declare no conflict of interest.

487 References

- 488 1. Lecker, B.; Illi, L.; Lemmer, A.; Oechsner, H. Biological hydrogen methanation – A review. *Bioresour. Technol.*
489 **2017**, *245*, 1220–1228.
- 490 2. Schiebahn, S.; Grube, T.; Robinius, M.; Tietze, V.; Kumar, B.; Stolten, D. Power to gas: Technological overview,
491 systems analysis and economic assessment for a case study in Germany. *Int. J. Hydrogen Energy* **2015**, *40*, 4285–
492 4294.
- 493 3. Luo, G.; Johansson, S.; Boe, K.; Xie, L.; Zhou, Q.; Angelidaki, I. Simultaneous hydrogen utilization and in situ
494 biogas upgrading in an anaerobic reactor. *Biotechnol. Bioeng.* **2012**, *109*, 1088–1094.
- 495 4. Verbeeck, K.; Buelens, L.C.; Galvita, V. V.; Marin, G.B.; Van Geem, K.M.; Rabaey, K. Upgrading the value of
496 anaerobic digestion via chemical production from grid injected biomethane. *Energy Environ. Sci.* **2018**, *11*, 1788–
497 1802.
- 498 5. Muñoz, R.; Meier, L.; Diaz, I.; Jeison, D. A review on the state-of-the-art of physical/chemical and biological
499 technologies for biogas upgrading. *Rev. Environ. Sci. Biotechnol.* **2015**, *14*, 727–759.
- 500 6. Angelidaki, I.; Treu, L.; Tsapekos, P.; Luo, G.; Campanaro, S.; Wenzel, H.; Kougias, P.G. Biogas upgrading and
501 utilization: Current status and perspectives. *Biotechnol. Adv.* **2018**, *36*, 452–466.

- 502 7. Villadsen, S.N.B.; Fosbøl, P.L.; Angelidaki, I.; Woodley, J.M.; Nielsen, L.P.; Møller, P. The Potential of Biogas;
503 The Solution to Energy Storage. *ChemSusChem* **2019**.
- 504 8. Rittmann, S.; Seifert, A.; Herwig, C. Essential prerequisites for successful bioprocess development of biological
505 CH₄ production from CO₂ and H₂. *Crit. Rev. Biotechnol.* **2015**, *35*, 141–151.
- 506 9. Hoelzle, R.D.; Virdis, B.; Batstone, D.J. Regulation mechanisms in mixed and pure culture microbial fermentation.
507 *Biotechnol. Bioeng.* **2014**, *111*, 2139–2154.
- 508 10. Kougias, P.G.; Treu, L.; Benavente, D.P.; Boe, K.; Campanaro, S.; Angelidaki, I. Ex-situ biogas upgrading and
509 enhancement in different reactor systems. *Bioresour. Technol.* **2017**, *225*, 429–437.
- 510 11. Rittmann, S.K.-M.R. A Critical Assessment of Microbiological Biogas to Biomethane Upgrading Systems. In
511 *Biogas Science and Technology*; Guebitz, G.M., Bauer, A., Bochmann, G., Gronauer, A., Weiss, S., Eds.; Springer
512 International Publishing: Cham, 2015; pp. 117–135 ISBN 978-3-319-21993-6.
- 513 12. Verstraete, W.; Wittebolle, L.; Heylen, K.; Vanparys, B.; de Vos, P.; van de Wiele, T.; Boon, N. Microbial
514 Resource Management: The road to go for environmental biotechnology. *Eng. Life Sci.* **2007**, *7*, 117–126.
- 515 13. Mu, D.S.; Liang, Q.Y.; Wang, X.M.; Lu, D.C.; Shi, M.J.; Chen, G.J.; Du, Z.J. Metatranscriptomic and comparative
516 genomic insights into resuscitation mechanisms during enrichment culturing. *Microbiome* **2018**, *6*, 1–15.
- 517 14. Garcia, S.L. Mixed cultures as model communities: Hunting for ubiquitous microorganisms, their partners, and
518 interactions. *Aquat. Microb. Ecol.* **2016**, *77*, 79–85.
- 519 15. Stewart, E.J. Growing unculturable bacteria. *J. Bacteriol.* **2012**, *194*, 4151–4160.
- 520 16. Kaeberlein, T.; Lewis, K.; Epstein, S.S. Quot; Microorganisms in Pure Culture in a Simulated Natural
521 Environment. *Sci. (New York, NY)* **2002**, *296*, 1127–1129.
- 522 17. Luo, G.; Angelidaki, I. Integrated biogas upgrading and hydrogen utilization in an anaerobic reactor containing
523 enriched hydrogenotrophic methanogenic culture. *Biotechnol. Bioeng.* **2012**, *109*, 2729–2736.
- 524 18. Savvas, S.; Donnelly, J.; Patterson, T.P.; Dinsdale, R.; Esteves, S.R. Closed nutrient recycling via microbial
525 catabolism in an eco-engineered self regenerating mixed anaerobic microbiome for hydrogenotrophic
526 methanogenesis. *Bioresour. Technol.* **2017**, *227*, 93–101.
- 527 19. Savvas, S.; Donnelly, J.; Patterson, T.; Chong, Z.S.; Esteves, S.R. Biological methanation of CO₂ in a novel biofilm
528 plug-flow reactor: A high rate and low parasitic energy process. *Appl. Energy* **2017**, *202*, 238–247.
- 529 20. Guneratnam, A.J.; Ahern, E.; FitzGerald, J.A.; Jackson, S.A.; Xia, A.; Dobson, A.D.W.; Murphy, J.D. Study of the
530 performance of a thermophilic biological methanation system. *Bioresour. Technol.* **2017**, *225*, 308–315.
- 531 21. Bassani, I.; Kougias, P.G.; Treu, L.; Porté, H.; Campanaro, S.; Angelidaki, I. Optimization of hydrogen dispersion
532 in thermophilic up-flow reactors for ex situ biogas upgrading. *Bioresour. Technol.* **2017**, *234*, 310–319.
- 533 22. Alfaro, N.; Fdz-Polanco, M.; Fdz-Polanco, F.; Díaz, I. Evaluation of process performance, energy consumption
534 and microbiota characterization in a ceramic membrane bioreactor for ex-situ biomethanation of H₂ and CO₂.
535 *Bioresour. Technol.* **2018**, *258*, 142–150.
- 536 23. Corbellini, V.; Kougias, P.G.; Treu, L.; Bassani, I.; Malpei, F.; Angelidaki, I. Hybrid biogas upgrading in a two-
537 stage thermophilic reactor. *Energy Convers. Manag.* **2018**, *168*, 1–10.
- 538 24. Yun, Y.M.; Sung, S.; Kang, S.; Kim, M.S.; Kim, D.H. Enrichment of hydrogenotrophic methanogens by means of
539 gas recycle and its application in biogas upgrading. *Energy* **2017**, *135*, 294–302.
- 540 25. Bassani, I.; Kougias, P.G.; Treu, L.; Angelidaki, I. Biogas Upgrading via Hydrogenotrophic Methanogenesis in
541 Two-Stage Continuous Stirred Tank Reactors at Mesophilic and Thermophilic Conditions. *Environ. Sci. Technol.*
542 **2015**, *49*, 12585–12593.
- 543 26. Rachbauer, L.; Beyer, R.; Bochmann, G.; Fuchs, W. Characteristics of adapted hydrogenotrophic community
544 during biomethanation. *Sci. Total Environ.* **2017**, *595*, 912–919.

- 545 27. Luo, G.; Angelidaki, I. Co-digestion of manure and whey for in situ biogas upgrading by the addition of H₂: Process
546 performance and microbial insights. *Appl. Microbiol. Biotechnol.* **2013**, *97*, 1373–1381.
- 547 28. Szuhaj, M.; Ács, N.; Tengölics, R.; Bodor, A.; Rákhely, G.; Kovács, K.L.; Bagi, Z. Conversion of H₂ and CO₂ to
548 CH₄ and acetate in fed-batch biogas reactors by mixed biogas community: a novel route for the power-to-gas
549 concept. *Biotechnol. Biofuels* **2016**, *9*, 102.
- 550 29. Mohd Yasin, N.H.; Maeda, T.; Hu, A.; Yu, C.P.; Wood, T.K. CO₂ sequestration by methanogens in activated
551 sludge for methane production. *Appl. Energy* **2015**, *142*, 426–434.
- 552 30. Rachbauer, L.; Voithl, G.; Bochmann, G.; Fuchs, W. Biological biogas upgrading capacity of a hydrogenotrophic
553 community in a trickle-bed reactor. *Appl. Energy* **2016**, *180*, 483–490.
- 554 31. Díaz, I.; Pérez, C.; Alfaro, N.; Fdz-Polanco, F. A feasibility study on the bioconversion of CO₂ and H₂ to
555 biomethane by gas sparging through polymeric membranes. *Bioresour. Technol.* **2015**, *185*, 246–253.
- 556 32. Voelklein, M.A.; Rusmanis, D.; Murphy, J.D. Biological methanation: Strategies for in-situ and ex-situ upgrading
557 in anaerobic digestion. *Appl. Energy* **2019**, *235*, 1061–1071.
- 558 33. Tian, H.; Fotidis, I.A.; Mancini, E.; Treu, L.; Mahdy, A.; Ballesteros, M.; González-Fernández, C.; Angelidaki, I.
559 Acclimation to extremely high ammonia levels in continuous biomethanation process and the associated microbial
560 community dynamics. *Bioresour. Technol.* **2018**, *247*, 616–623.
- 561 34. Nikolausz, M.; Walter, R.F.H.; Sträuber, H.; Liebetrau, J.; Schmidt, T.; Kleinstüber, S.; Bratfisch, F.; Günther,
562 U.; Richnow, H.H. Evaluation of stable isotope fingerprinting techniques for the assessment of the predominant
563 methanogenic pathways in anaerobic digesters. *Appl. Microbiol. Biotechnol.* **2013**, *97*, 2251–2262.
- 564 35. Lv, Z.; Leite, A.F.; Harms, H.; Glaser, K.; Liebetrau, J.; Kleinstüber, S.; Nikolausz, M. Microbial community
565 shifts in biogas reactors upon complete or partial ammonia inhibition. *Appl. Microbiol. Biotechnol.* **2019**, *103*, 519–
566 533.
- 567 36. Porsch, K.; Wirth, B.; Tóth, E.M.; Schattenberg, F.; Nikolausz, M. Characterization of wheat straw-degrading
568 anaerobic alkali-tolerant mixed cultures from soda lake sediments by molecular and cultivation techniques. *Microb.*
569 *Biotechnol.* **2015**, *8*, 801–814.
- 570 37. Bonk, F.; Popp, D.; Weinrich, S.; Sträuber, H.; Becker, D.; Kleinstüber, S.; Harms, H.; Centler, F. Determination
571 of Microbial Maintenance in Acetogenesis and Methanogenesis by Experimental and Modeling Techniques. *Front.*
572 *Microbiol.* **2019**, *10*, 1–13.
- 573 38. Klindworth, A.; Pruesse, E.; Schweer, T.; Peplies, J.; Quast, C.; Horn, M.; Glöckner, F.O. Evaluation of general
574 16S ribosomal RNA gene PCR primers for classical and next-generation sequencing-based diversity studies.
575 *Nucleic Acids Res.* **2013**, *41*, e1.
- 576 39. Steinberg, L.M.; Regan, J.M. Phylogenetic comparison of the methanogenic communities from an acidic,
577 oligotrophic fen and an anaerobic digester treating municipal wastewater sludge. *Appl. Environ. Microbiol.* **2008**,
578 *74*, 6663–6671.
- 579 40. Martin, M. Cutadapt removes adapter sequences from high-throughput sequencing reads kenkyuhi hojokin gan
580 rinsho kenkyu jigyo. *EMBnet.journal* **2013**, *17*, 10–12.
- 581 41. Bolyen, E.; Rideout, J.R.; Dillon, M.R.; Bokulich, N.A.; Abnet, C.C.; Al-Ghalith, G.A.; Alexander, H.; Alm, E.J.;
582 Arumugam, M.; Asnicar, F.; et al. Reproducible, interactive, scalable and extensible microbiome data science using
583 QIIME 2. *Nat. Biotechnol.* **2019**, *37*, 852–857.
- 584 42. Callahan, B.J.; McMurdie, P.J.; Rosen, M.J.; Han, A.W.; Johnson, A.J.A.; Holmes, S.P. DADA2: High-resolution
585 sample inference from Illumina amplicon data. *Nat. Methods* **2016**, *13*, 581–583.
- 586 43. McIlroy, S.J.; Kirkegaard, R.H.; McIlroy, B.; Nierychlo, M.; Kristensen, J.M.; Karst, S.M.; Albertsen, M.; Nielsen,
587 P.H. MiDAS 2.0: An ecosystem-specific taxonomy and online database for the organisms of wastewater treatment

- 588 systems expanded for anaerobic digester groups. *Database* **2017**, 2017, 1–9.
- 589 44. Fish, J.A.; Chai, B.; Wang, Q.; Sun, Y.; Brown, C.T.; Tiedje, J.M.; Cole, J.R. FunGene: The functional gene
590 pipeline and repository. *Front. Microbiol.* **2013**, *4*, 1–14.
- 591 45. RStudio Team RStudio: Integrated Development Environment for R 2016.
- 592 46. Rcoreteam R: A language and environment for statistical computing. R Foundation for Statistical Computing 2019.
- 593 47. Wickham, H. ggplot2: Elegant Graphics for Data Analysis 2016.
- 594 48. Kern, T.; Theiss, J.; Röske, K.; Rother, M. Assessment of hydrogen metabolism in commercial anaerobic digesters.
595 *Appl. Microbiol. Biotechnol.* **2016**, *100*, 4699–4710.
- 596 49. Shieh, J.S.; Whitman, W.B. Pathway of acetate assimilation in autotrophic and heterotrophic methanococci. *J.*
597 *Bacteriol.* **1987**, *169*, 5327–5329.
- 598 50. Goyal, N.; Padhiary, M.; Karimi, I.A.; Zhou, Z. Flux measurements and maintenance energy for carbon dioxide
599 utilization by *Methanococcus marisaludis*. *Microb. Cell Fact.* **2015**, *14*, 1–9.
- 600 51. Feist, A.M.; Scholten, J.C.M.; Palsson, B.; Brockman, F.J.; Ideker, T. Modeling methanogenesis with a genome-
601 scale metabolic reconstruction of *Methanosarcina barkeri*. *Mol. Syst. Biol.* **2006**, *2*, 1–14.
- 602 52. Treu, L.; Campanaro, S.; Kougias, P.G.; Sartori, C.; Bassani, I.; Angelidaki, I. Hydrogen-fueled microbial
603 pathways in biogas upgrading systems revealed by genome-centric metagenomics. *Front. Microbiol.* **2018**, *9*, 1–
604 16.
- 605 53. Jensen, M.B.; Strübing, D.; de Jonge, N.; Nielsen, J.L.; Ottosen, L.D.M.; Koch, K.; Kofoed, M.V.W. Stick or leave
606 – Pushing methanogens to biofilm formation for ex situ biomethanation. *Bioresour. Technol.* **2019**, *291*, 121784.
- 607 54. Dupnock, T.L.; Deshusses, M.A. High-Performance Biogas Upgrading Using a Biotrickling Filter and
608 Hydrogenotrophic Methanogens. *Appl. Biochem. Biotechnol.* **2017**, 1–15.
- 609 55. Schuchmann, K.; Müller, V. Autotrophy at the thermodynamic limit of life: A model for energy conservation in
610 acetogenic bacteria. *Nat. Rev. Microbiol.* **2014**, *12*, 809–821.
- 611 56. Westerholm, M.; Moestedt, J.; Schnürer, A. Biogas production through syntrophic acetate oxidation and deliberate
612 operating strategies for improved digester performance. *Appl. Energy* **2016**, *179*, 124–135.
- 613 57. Diekert, G.; Wohlfarth, G. Metabolism of homoacetogens. *Antonie Van Leeuwenhoek* **1994**, *66*, 209–221.
- 614 58. Ljungdahl, L. The Autotrophic Pathway of Acetate Synthesis in Acetogenic Bacteria. *Annu. Rev. Microbiol.* **1986**,
615 *40*, 415–450.
- 616 59. Bengelsdorf, F.R.; Beck, M.H.; Erz, C.; Hoffmeister, S.; Karl, M.M.; Riegler, P.; Wirth, S.; Poehlein, A.; Weuster-
617 Botz, D.; Dürre, P. Bacterial Anaerobic Synthesis Gas (Syngas) and CO₂ + H₂ Fermentation. *Adv. Appl. Microbiol.*
618 **2018**, *103*, 143–221.
- 619 60. Peng, J.; Wegner, C.E.; Bei, Q.; Liu, P.; Liesack, W. Metatranscriptomics reveals a differential temperature effect
620 on the structural and functional organization of the anaerobic food web in rice field soil. *Microbiome* **2018**, *6*, 1–
621 16.
- 622 61. Mosbæk, F.; Kjeldal, H.; Mulat, D.G.; Albertsen, M.; Ward, A.J.; Feilberg, A.; Nielsen, J.L. Identification of
623 syntrophic acetate-oxidizing bacteria in anaerobic digesters by combined protein-based stable isotope probing and
624 metagenomics. *ISME J.* **2016**, *10*, 2405–2418.
- 625 62. De Vrieze, J.; Boon, N.; Verstraete, W. Taking the technical microbiome into the next decade. *Environ. Microbiol.*
626 **2018**, *20*, 1991–2000.
- 627 63. Stams, A.J.M.; Van Dijk, J.B.; Dijkema, C.; Plugge, C.M. Growth of syntrophic propionate-oxidizing bacteria with
628 fumarate in the absence of methanogenic bacteria. *Appl. Environ. Microbiol.* **1993**, *59*, 1114–1119.
- 629 64. Schink, B.; Montag, D.; Keller, A.; Müller, N. Hydrogen or formate: Alternative key players in methanogenic
630 degradation. *Environ. Microbiol. Rep.* **2017**, *9*, 189–202.

- 631 65. Woods, D.D. Hydrogenlyases: The synthesis of formic acid by bacteria. *Biochem. J.* **1936**, *30*, 515–51527.
- 632 66. Peters, V.; Janssen, P.H.; Conrad, R. Transient production of formate during chemolithotrophic growth of
633 anaerobic microorganisms on hydrogen. *Curr. Microbiol.* **1999**, *38*, 285–289.
- 634 67. Wu, W.M.; Hickey, R.F.; Jain, M.K.; Zeikus, J.G. Energetics and regulations of formate and hydrogen metabolism
635 by *Methanobacterium formicicum*. *Arch. Microbiol.* **1993**, *159*, 57–65.
- 636 68. Wintsche, B.; Glaser, K.; Sträuber, H.; Centler, F.; Liebetrau, J.; Harms, H.; Kleinstüber, S. Trace elements induce
637 predominance among methanogenic activity in anaerobic digestion. *Front. Microbiol.* **2016**, *7*.
- 638 69. Agnessens, L.M.; Ottosen, L.D.M.; Voigt, N.V.; Nielsen, J.L.; de Jonge, N.; Fischer, C.H.; Kofoed, M.V.W. In-
639 situ biogas upgrading with pulse H₂ additions: The relevance of methanogen adaption and inorganic carbon level.
640 *Bioresour. Technol.* **2017**, *233*, 256–263.
- 641 70. Savvas, S.; Donnelly, J.; Patterson, T.; Chong, Z.S.; Esteves, S.R. Methanogenic capacity and robustness of
642 hydrogenotrophic cultures based on closed nutrient recycling via microbial catabolism: Impact of temperature and
643 microbial attachment. *Bioresour. Technol.* **2018**, *257*, 164–171.